

An Experimental Study of Turbulence in Northern Suburban Surface Layer of Beijing

Su Hongbing(苏红兵)* and Hong Zhongxiang(洪钟祥)
(LAPC, Institute of Atmospheric Physics, Chinese Academy of Sciences, Beijing 100029)

Manuscript received June 17, 1993; revised September 29, 1993.

Based upon the data of three orthogonal wind velocity components and sound temperature measured by two FA-11 ultrasonic anemometer / thermometers fixed at 47m and 120m of the Beijing 325m meteorological tower, this paper presents the statistical turbulent characteristics and their diurnal variations in the surface layer over a rough and complex terrain near the northern outskirts of Beijing. Especially, the nondimensional variances of the vertical velocity and sound temperature and their variations with the stability, the normalized velocity component and temperature spectra and cospectra are calculated and compared with the results observed over uniform areas.

Key words: surface layer; ultrasonic anemometer / thermometer; atmospheric turbulence.

1. INTRODUCTION

The understanding of the turbulent characteristics in the atmospheric boundary layer, especially in the surface layer, in urban and suburban areas, is very important for the studies of urban climate, environment protection, the transport and diffusion of pollutants, etc., in these areas as known for their large population.

As one of the main approaches to study the atmospheric turbulence, the observations and the statistical analyses of the measurements can describe certain properties of atmospheric turbulence from relatively accessible quantities, such as the wind speed and temperature, etc.

Several major measurement programs have been carried out over uniform terrain since 1964 and provided us with a systematic understanding of the turbulent characteristic over the uniform terrain. Especially, the results of the Kansas experiment demonstrated that Monin-Obukhov similarity theory provided a rational method to describe the turbulent characteristics in the surface layer. However, it has been doubted whether this theory is applicable to describing the atmospheric turbulence over heterogeneous and complex terrain since

* Present address: Atmospheric Science, Land, air and Water Resources, University of California, Davis, CA 95616-8627, U. S. A.

there have not been many systematic measurements over complex terrain which might have some local characteristics.

The Beijing 325m meteorological tower^[1] is located near the northern outskirts of Beijing city. According to Zhang et al.^[2], two heights, 47m and 120m were chosen for this experiment. The 120m height was chosen as a comparison to 47m height because an up-level inversion around 120m has been frequently observed from the temperature profiles in this area.

Sonic anemometer / thermometer is an important tool for the measurement of the atmospheric turbulence. However, they were usually applied only for measuring the wind speed fluctuations. Modern sonic anemometer / thermometer can also measure of temperature fluctuations. Schotanus et al.^[3], showed how to eliminate the effects of cross-wind and humidity from the temperature statistics measured by the sonic anemometer-thermometer with simultaneous measurements of momentum flux and humidity flux. Kaimal et al.^[4], also discussed the distinct advantages of the sonic thermometry, such as compatibility in spatial and temporal resolution with the vertical wind component, collocation of the two sampling volumes, predictable calibration, unaffected by aging or atmospheric contamination, freedom from "cold spikes" resulting from salt deposition for marine applications as platinum wire and other immersion-type sensor suffer.

In our experiment, two FA-11 ultrasonic anemometer / thermometers developed by the Institute of Atmospheric Physics, Chinese Academy of Sciences, were used at 47m and 120m of the 325m Beijing meteorological tower, respectively, to measure the three orthogonal wind components and the sound temperature.

2. DATA COLLECTION AND PREPROCESSING

Su^[5] gave the details about the installation of the instruments and the sampling of the data. The sampling rate of the FA-11 ultra sonic anemometer-thermometer is 22 per second. Data collected during the periods from 1:48 a.m., March 27, 1992 to 0:44 a.m., March 28, 1992; and from 1:44 p.m., April 13, 1992 to 12:40 p.m., April 14, 1992 (Beijing local time), were used for the analyses in this paper. Su^[5] also gave the details about the preprocessing of the raw data, including the detection and correction of "wild points", corrections of the sound distances and the contamination of the cross-wind to the sound temperature.

The sound temperature T_{vs} ^[6] measured by FA-11 sonic anemometer / thermometer is given as,

$$T_{vs} = (1 + 0.518q)T = (1 + 0.322\frac{e}{p})T, \quad (1)$$

where T is absolute temperature in Kelvin, q is specific humidity, p is pressure and e is water vapor pressure.

The sound temperature T_{vs} and the adiabatic sound speed c_s , have the following approximate relation^[7],

$$c_s = (\gamma_a R_a T_{vs})^{1/2} \approx 20.067 T_{vs}^{1/2}, \quad (2)$$

where γ_a is the ratio of specific heat at constant pressure to that at constant volume of dry air, R_a is the gas constant for dry air.

The meteorological definition of the atmospheric virtual temperature T_v is,

$$T_v = (1 + 0.608q)T = (1 + 0.378\frac{e}{p})T. \quad (3)$$

From Eqs.(1) and (3), we can see that the sound temperature T_{vs} and the virtual temperature T_v are different, although they are very close.

3. ESTIMATES OF TURBULENT CHARACTERISTIC PARAMETERS

3.1 Averaging Time

The determination of the length of averaging time is a basic but important problem in the statistical analysis of the observation of the atmospheric turbulence. According to the analyses of Lumley and Panofsky⁽⁸⁾, Wyngaard⁽⁹⁾, Haugen⁽¹⁰⁾ and Roth⁽¹¹⁾, also for the convenience of data processing, we used an averaging time of 84 minutes.

3.2 Calculation of Horizontal Wind Speed and Direction

The scalar mean horizontal wind speed u_s , azimuth φ_s and the vector mean horizontal wind speed u_v , azimuth φ_v are expressed as,

$$\begin{cases} u_s = \bar{v} = \sqrt{\bar{v}_x^2 + \bar{v}_y^2}, \\ \varphi_s = \bar{\varphi} = \arctg\left(\frac{\bar{v}_y}{\bar{v}_x}\right), \end{cases} \quad (4)$$

and

$$\begin{cases} u_v = \sqrt{\bar{v}_x'^2 + \bar{v}_y'^2}, \\ \varphi_v = \arctg\left(\frac{\bar{v}_y'}{\bar{v}_x'}\right). \end{cases} \quad (5)$$

For uniform turbulence, Frenkiel⁽¹²⁾ gave,

$$u_s \approx u_v \left[1 + \frac{1}{2} \left(\frac{\sigma_v}{u_v} \right)^2 \right] \equiv u_c, \quad (6)$$

where σ_v is the variance of the lateral wind component v .

Figure 1 gives the comparisons between u_s and u_v , u_s and u_c , φ_s and φ_v . It shows that the observed data meet Eq.(6) very well. However, in many cases, φ_s and φ_v are very different. In such cases, it should be careful in determining the dominant wind direction.

3.3 Coordinate Transform and Detrending

The x -axis for coordinate transform to make the mean lateral wind component equal zero ($\bar{v} = 0$), and its fluctuation is equal to its instantaneous value, $v' = v$.

However, in many cases, we found that $\overline{v'w'} \geq \overline{u'w'}$, which showed the mean horizontal wind and the horizontal component of the Reynolds stress are not in the same direction. This maybe due to the effects of the complex terrain of this area, diurnal variation and local circulation, etc. Therefore, some researchers suggested the linear trends of horizontal wind direction be used rather than its mean for the coordinate transform to meet both $\bar{v} = 0$ and $\overline{v'w'} \leq \overline{u'w'}$.

In this paper, we did not use the above empirical method in the coordinate transform. Instead, we still used the conventional mean horizontal wind direction for coordinate transform. However, the contributions to the friction velocity u_* from both $\overline{v'w'}$ and $\overline{u'w'}$ were included.

After coordinate transform, only linear trends were eliminated from the time series of the three orthogonal wind components and the sound temperature.

3.4 Characteristic Turbulent Parameters in the Surface Layer

According to the Monin-Obukhov similarity, the characteristic scaling parameters in the surface layer are friction velocity u_* , characteristic temperature scale T_* , Monin-Obukhov

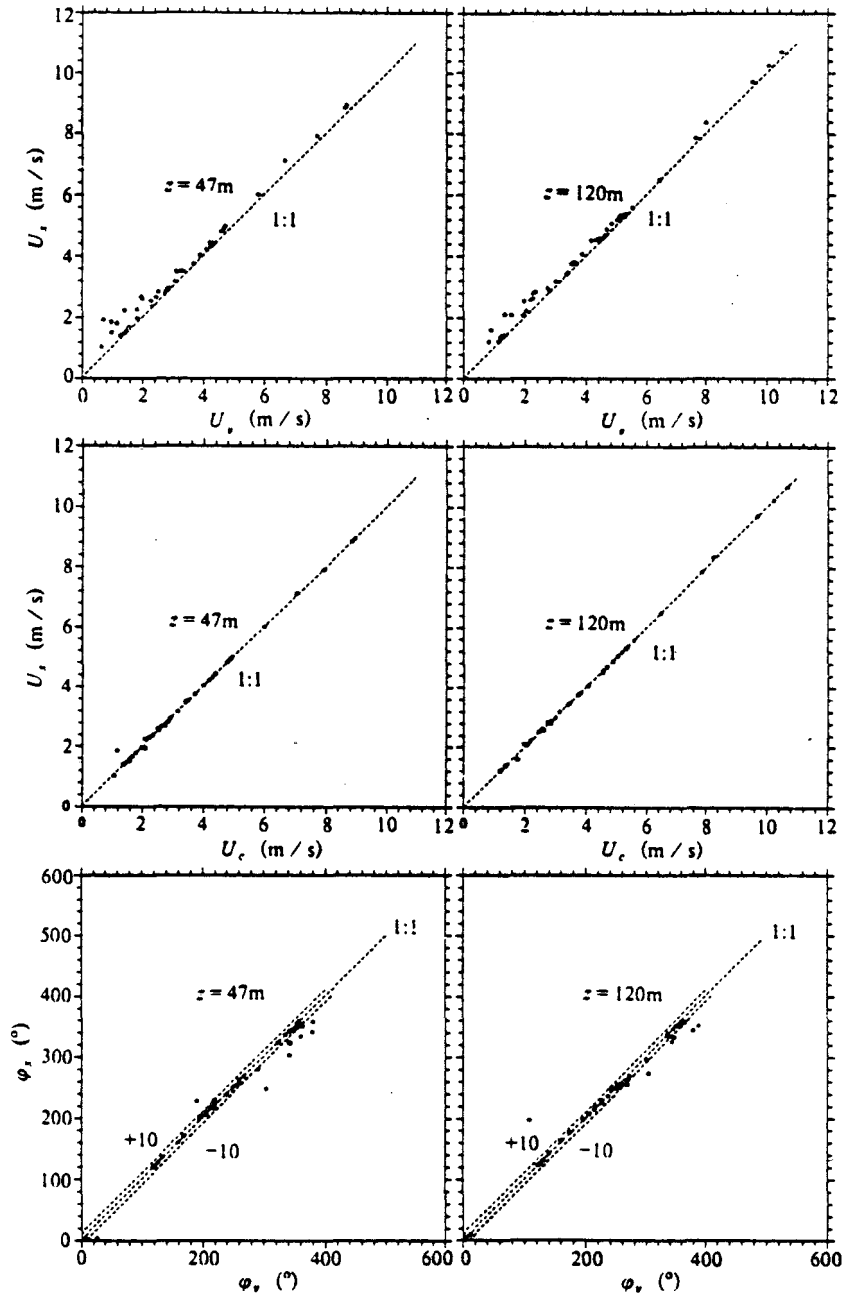


FIGURE 1. Scalar and vector averaged horizontal wind speed and azimuth at 47 m and 120 m.

length L , height from the surface z , roughness z_0 and zero-displacement distance d .

When humidity is considered, the characteristic virtual temperature T_{v*} is used instead of T_* .^[13]

$$\overline{w'T'_v} \approx \overline{w'T'} + 0.61\overline{T} \overline{w'q'}, \tag{7}$$

$$T_{v.} \approx T. + 0.61\overline{T}q., \tag{8}$$

where $T_{v.}$, $T.$ and $q.$ are defined as follows.

$$T_{v.} = -\frac{\overline{w'T'_v}}{u.}, \quad T. = -\frac{\overline{w'T'}}{u.}, \quad q. = -\frac{\overline{w'q'}}{u.} \tag{9}$$

From Eqs. (1) and (3), we know that the sound temperature T_{vs} is a good approximation of the virtual temperature T_v . Then, we used the following formulae to calculate the characteristic parameters.

$$\begin{cases} u. = [|\overline{u'w'}|^2 + |\overline{v'w'}|^2]^{1/4}, & T_{v.} \approx -\frac{\overline{w'T'_{vs}}}{u.}, \\ L \approx -\frac{\overline{T_{vs}}u.^3}{\kappa g \overline{w'T'_{vs}}}, & \zeta \approx \frac{z-d}{L}, \\ d = 3.13 \text{ m}, & z_0 = 0.63 \text{ m}, \end{cases} \tag{10}$$

where $\kappa = 0.4$ is the von Karman constant, g is gravity.

Figure 2 gives the diurnal variations (from 1:48 a.m., March 27 to 0:44 a.m., March 28, 1992) of turbulent intensities i_u, i_v, i_z , mean turbulent kinematic energy TKE , mean eddy heat flux Q_h , friction velocity $u.$, characteristic virtual temperature $T_{v.}$ and stability ζ . i_u, i_v, i_z, TKE , and Q_h are defined as follows.

$$i_x = \sigma_x / u_x, \quad i_y = \sigma_y / v_u, \quad i_z = \sigma_w / u_w, \tag{11}$$

$$TKE = \bar{e} = \frac{1}{2}(\overline{u'^2} + \overline{v'^2} + \overline{w'^2}) \tag{12}$$

$$Q_h = \rho c_p \overline{w'T'_{vs}}, \tag{13}$$

From Figure 2, we can see that the above characteristic parameters at 47m are very close to those at 120m for most of the time during the diurnal process, which shows that the two heights are in the same characteristic layer for most of the time. Moreover, the maximum turbulent intensities appear between 10 and 12 a.m. while maximum TKE appear between 1 to 4 p.m. This is because the turbulent intensities are determined by both the variances of the velocity components and the mean horizontal wind speed, while TKE only depends on the velocity variances. In addition, the mean horizontal wind speed during 1 to 4 p.m. is usually much greater than that during 10 to 12 a.m.

We can also see that the friction velocity at 120m is greater than that at 47m for most of the time. The eddy heat flux at 120m is also greater than that at 47m during 12 to 6 p.m. This maybe due to the complex terrain around the meteorological tower which can lead to the formation of internal boundary layer.

3.5 Nondimensional Variance of Wind Components and Sound Temperature

Monin-Obukhov similarity indicates that in the surface layer, the variances of wind components and temperature which are nondimensionalized by friction velocity and characteristic temperature, respectively, are only functions of stability, i.e.,

$$\frac{\sigma_x}{u.} = \Phi_x(\zeta), \quad x = u, v, w, \tag{14}$$

$$\sigma_{T_v} / |T_{v.}| = \Phi_{T_v}(\zeta). \tag{15}$$

And in neutral condition, we have,

$$\sigma_u = Au., \quad \sigma_v = Bu., \quad \sigma_w = Cu., \tag{16}$$

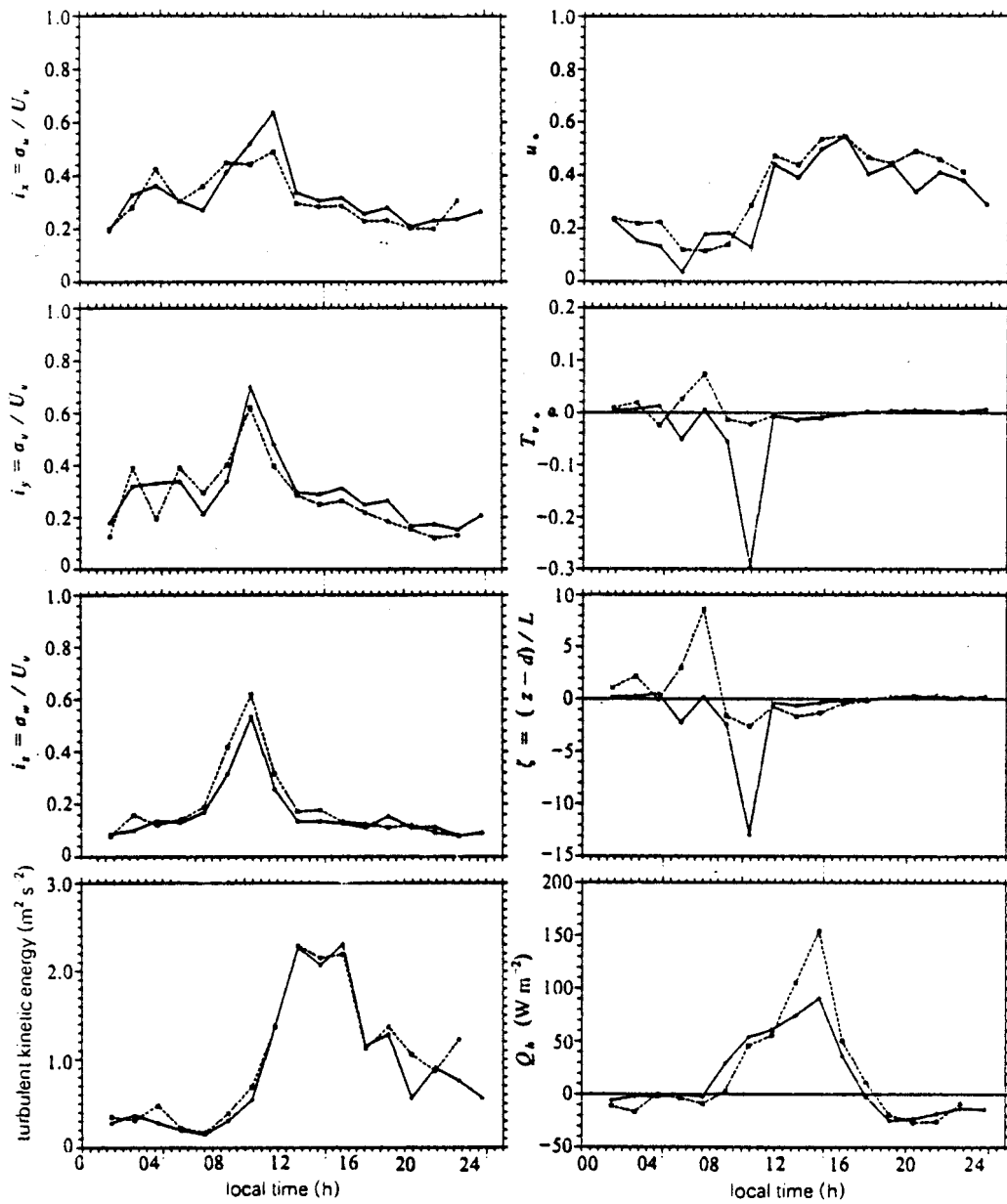


FIGURE 2. Diurnal variations of turbulent characteristic parameters at 47 m and 120 m.

where A , B , C are constants. Panofsky and Dutton^[14] gave the average values of A , B , C over various surfaces as $A = 2.4$, $B = 1.9$, $C = 1.25$.

They also gave the empirical formula for the variances of the vertical velocity component and the temperature as functions of the stability, respectively.

$$\Phi_w(\zeta) = \begin{cases} 1.25(1 - 3\zeta)^{1/3}, & \zeta < 0, \\ 1.25, & \zeta \geq 0. \end{cases} \quad (17)$$

and

$$\Phi_{T_v}(\zeta) = 5(1 - 16\zeta)^{-1/2}, \quad \zeta < 0. \quad (18)$$

By averaging σ_w / u_* , σ_v / u_* and σ_w / u_* in the stability range of $-0.1 < \zeta < 0.1$, we got $A = 2.33$, $B = 1.97$ and $C = 1.16$ which agreed very well with the mean values given by Panofsky. Zhang et al.^[2] gave $A = 2.30$, $B = 1.62$ and $C = 1.237$ for the same area. Their A and C values agreed very well with our results but B is less than the B we got.

Figure 3 gives σ_w / u_* and $\sigma_{T_v} / |T_v^*|$ varying with stability in the range of $-4.0 < \zeta < 4.0$. Compared with the empirical formula suggested by Panofsky and Dutton^[14], we found the formulae (17) and (18) matched our data very well. This may be due to the fact that the vertical eddy size is relatively small and can adjust to the complex surface very fast.

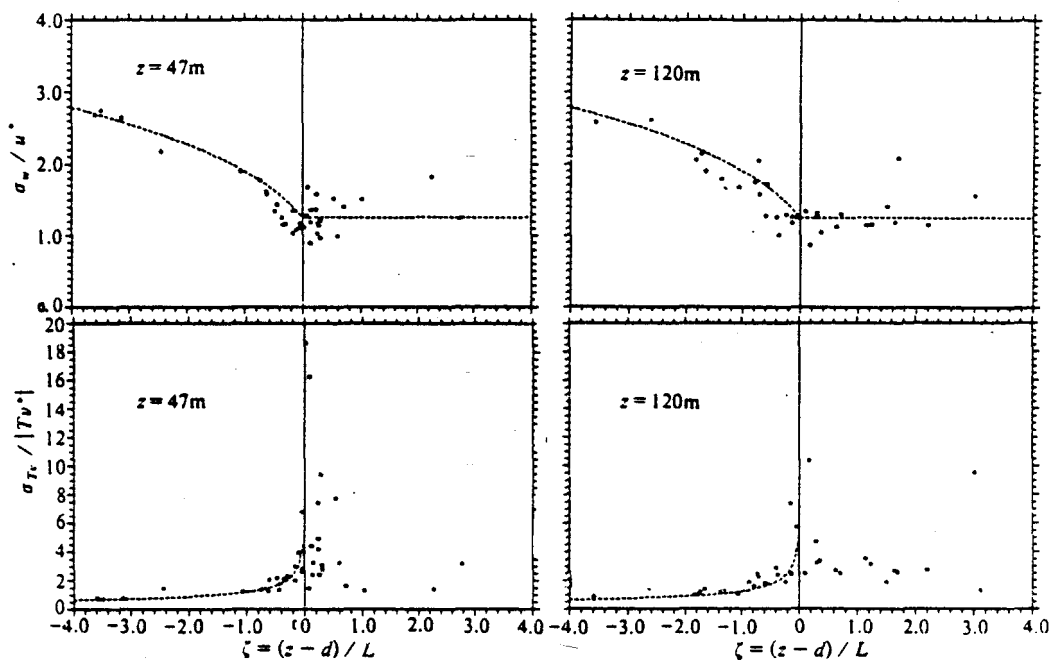


FIGURE 3. Variations of nondimensional variances of vertical velocity and sound temperature with stability ζ .

However, in stable conditions, the data are much more scattering because σ_w , u_* and T_v^* are very small and the measurement accuracy is limited.

4. SPRCTEA AND COSPECTRA IN THE SURFACE LAYER

In the surface layer, the dimensionless spectral and cospectral densities also follow the Monin-Obukhov similarity. All spectral functions in the inertial subrange can be expressed in the following dimensionless form^[13]

$$\begin{cases} \frac{nS_u(n)}{u_*^2} = \frac{\alpha_u}{(2\pi\kappa)^{2/3}} \varphi_\varepsilon^{2/3} f^{-2/3}, \\ \frac{nS_v(n)}{u_*^2} = \frac{\alpha_v}{(2\pi\kappa)^{2/3}} \varphi_\varepsilon^{2/3} f^{-2/3}, \\ \frac{nS_w(n)}{u_*^2} = \frac{\alpha_w}{(2\pi\kappa)^{2/3}} \varphi_\varepsilon^{2/3} f^{-2/3}, \\ \frac{nS_T(n)}{T_*^2} = \frac{\alpha_T}{(2\pi\kappa)^{2/3}} \varphi_\varepsilon^{1/3} \varphi_N f^{-2/3}, \end{cases} \quad (19)$$

where $i = u, v, w$, and

$$\begin{cases} -\frac{nC_{uw}(n)}{u_*^2} = \frac{\alpha_{uw}}{(2\pi\kappa)^{4/3}} \varphi_\varepsilon^{1/3} \varphi_m f^{-4/3}, \\ -\frac{nC_{wT}(n)}{u_* T_*} = \frac{\alpha_{wT}}{(2\pi\kappa)^{4/3}} \varphi_\varepsilon^{1/3} \varphi_h f^{-4/3}, \\ \frac{nC_{uT}(n)}{u_* T_*} = \frac{\alpha_{uT}}{(2\pi\kappa)^{3/2}} \varphi_\varepsilon^{1/4} \varphi_m^{1/4} \varphi_h f^{-3/2}, \end{cases} \quad (20)$$

where n is frequency, $f = nz / u_*$ is nondimensional frequency, κ is von Karman constant, φ_ε is nondimensional dissipation rate for turbulent energy, φ_N is nondimensional dissipation rate for temperature fluctuations, φ_m is nondimensional wind shear and φ_h is nondimensional temperature gradient. All of them are universal similarity functions of stability ζ . α is Kolmogoroff constant. Kaimal et al.^[15] gave $\alpha_u = 0.5$, $\alpha_v = \alpha_w = 4\alpha_u / 3$, $\alpha_T = 0.8$. Wyngaard and Cot gave $\alpha_{uw} = 0.12$, $\alpha_{wT} = 0.20$. Hgstrm summarized the values of α_u from various sources and gave his estimate as $\alpha_u = 0.62 \pm 0.08$.

In order to show the normalized spectral and cospectral density varying with stability ζ , we rewrote Eqs.(19) and (20) as follows

$$\begin{cases} \frac{nS_u(n)}{u_*^2} = G_u(\alpha_u, \zeta) f^{-2/3}, \\ \frac{nS_v(n)}{u_*^2} = G_v(\alpha_v, \zeta) f^{-2/3}, \\ \frac{nS_w(n)}{u_*^2} = G_w(\alpha_w, \zeta) f^{-2/3}, \\ \frac{nS_T(n)}{T_*^2} = G_T(\alpha_T, \zeta) f^{-2/3}, \end{cases} \quad (21)$$

and

$$\begin{cases} -\frac{nC_{uw}(n)}{u_*^2} = G_{uw}(\alpha_{uw}, \zeta) f^{-4/3}, \\ -\frac{nC_{wT}(n)}{u_* T_*} = G_{wT}(\alpha_{wT}, \zeta) f^{-4/3}, \\ \frac{nC_{uT}(n)}{u_* T_*} = G_{uT}(\alpha_{uT}, \zeta) f^{-3/2}. \end{cases} \quad (22)$$

For the inertial subrange, we can get the G factors which are functions of α and ζ . If the G factors are also removed to the left-hand sides of equation sets (21) and (22), the spectral curves for different ζ should coincide together.

Figure 4 gives the near neutral normalized spectra and cospectra at both 47m and 120m. For the energy spectra of the three wind components, we can see that there exist the “ $-2/3$

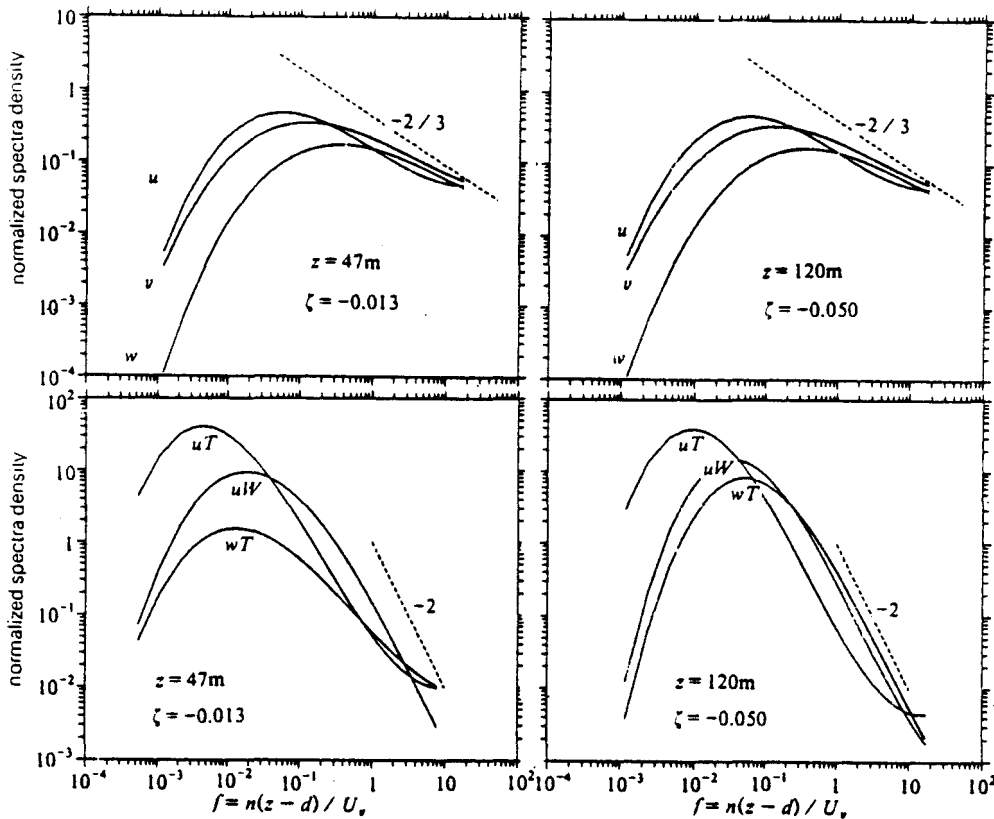


FIGURE 4. Near neutral normalized spectra and cospectra.

power law" in the inertial subrange and the peak frequencies follow $f_{u\max} < f_{v\max} < f_{w\max}$, which shows the energy-containing eddy size increases in the order from vertical to lateral and then to longitudinal directions. For most of the cospectra, the slopes in the inertial subrange are close to "-2 power law". The peak frequencies follow $f_{uw\max} \approx f_{wT\max} > f_{uT\max}$. In the inertial subrange, $C_{wT} > C_{uT}$, which shows small eddies are more efficient in transporting heat vertically than horizontally. On the other hand, for low frequencies, $C_{wT} \ll C_{uT}$, which shows large eddies transport heat more efficiently in the horizontal direction than in the vertical direction. In the high frequencies of the cospectra for heat flux, we can see the spectra of "white noise" which is due to the limited resolution of the FA-11 ultrasonic anemometer-thermometer for the measurement of temperature fluctuations which are very small in neutral condition.

Figure 5 gives the variance spectra of the wind components and the sound temperature. In the inertial subrange, the spectra curves coincide very well and are close to "-2/3 power law". In low frequencies, the spectral curves expand for different stabilities. Moreover, the vertical velocity spectral density decreases much faster than the two horizontal wind component spectral densities when the frequency decreases, which shows the vertical turbulent kinetic energy is mainly from small eddies.

Similarly, Figure 6 gives the cospectra which coincide very well in the inertial subrange and expand with ζ in the low frequencies. In the inertial subrange, Kaimal et al.^[15] gave nC_{uw} and nC_{wT} following "-4/3 power law" and nC_{uT} following "-3/2 power law". However,

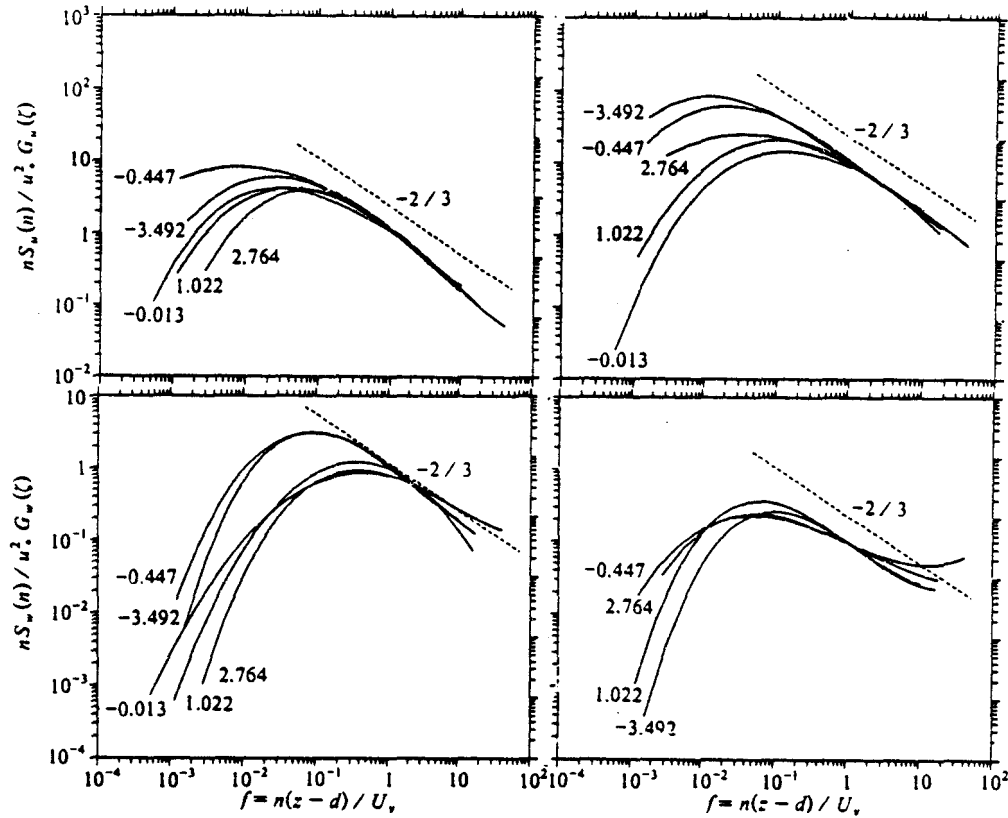


FIGURE 5. Normalized variance spectra of three wind components and sound temperature.

our results gave all the cospectra following “-2 power law”.

5. CONCLUSION

1) In this experiment, the characteristic turbulent parameters at 47 m and 120 m were very close for most of the time of the diurnal process which showed that these two heights were usually in the same characteristic layer. The friction velocity at 120m being greater than that at 47m showed the possibility of the existence of urban internal boundary layer due to the complex surface conditions.

2) The nondimensional variances of the vertical velocity and the sound temperature at both 47m and 120m followed the Monin-Obukhov similarity very well and matched the empirical formula suggested by Panofsky and Dutton^[14]. In neutral condition, the variances of the three wind components were also close to the constants given by Panofsky and Dutton^[14].

3) The normalized variance spectra followed the “-2/3 power law” in the inertial subrange. However, only u and v spectra varied with stability ζ in the low frequencies as given by Kaimal et al.^[15]. The slope of the cospectra in the inertial subrange followed “-2 power law” rather than “-4/3 or -3/2 power law” as given by Kaimal et al.^[15]. Due to the limited data obtained in this experiment, whether or not the above difference represents the characteristics of turbulence in the surface layer over the local complex surface remains to be verified by more systematic observations.

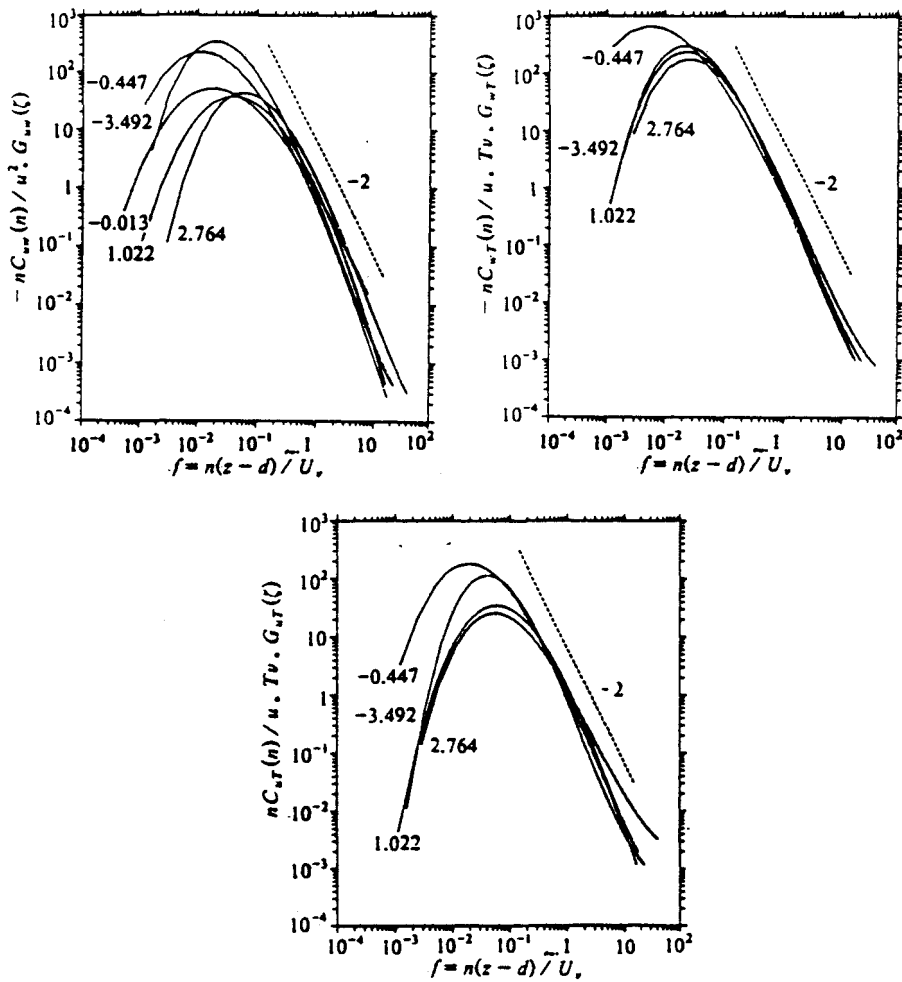


FIGURE 6. Normalized cospectral variations with stability ζ .

ACKNOWLEDGEMENT

The authors would like to express their deep appreciation to Zhao Yijun and Luo Weidong for their help in carrying out the experiment. We also would like to thank Professors Zhang Aichen, Liu Shida and Pan Naixian of Peking University for their helpful discussion with us. This experimental work was partially supported by the State Key Laboratory of Atmospheric Physics and Atmospheric Chemistry, Institute of the Atmospheric Physics, Chinese Academy of Sciences.

REFERENCES

- [1] Hong Zhongxiang, 1983: Beijing Meteorological Tower, *The Measuring System of Beijing 325m Meteorological Tower*, Science Press, 1-7. (in Chinese)
- [2] Zhang Aichen, Lu Jic, Zhang Bing and Liu Shuhua, 1991: The turbulence characteristics in the boundary layer of the rural area and border of urban area of Beijing, *Scientia Atmospherica Sinica*, 15, No.4, 87-96. (in Chinese)
- [3] Schotanus, P., Nicuwstadt, F.T.M. and H.A.R. De Briun, 1983: Temperature measurement with a sonic anemometer and its application to heat and moisture fluxes, *Boundary-Layer Meteorol.*, 26, 81-93.

- [5] Su Hongbing, 1992, FA-11 Ultrasonic Anemometer-Thermometer and Its Application for the Measurement of the Atmospheric Turbulence, Thesis for the Degree of Master's Science, Institute of Atmospheric Physics, Chinese Academy of Sciences. (in Chinese)
- [6] Marillierm, A., Cabane M. and D. Cruette, 1991: Notes and correspondence — preliminary tests of an ultrasonic thermoanemometer for aircraft measurements, *J. Atmos. and Oceanic Tech.*, **8**, 597-605.
- [7] Holton, J. R., 1993: *An Introduction to Dynamic Meteorology*, 3rd ed., Academic Press, 190-193.
- [8] Lumley, J. L. and H. A. Panofsky, 1964: *The Structure of Atmospheric Turbulence*, Interscience Publish, New York, 239.
- [9] Wyngaard, J. C., 1973: On surface layer turbulence, *Workshop on Micrometeorology*, AMS, 135-141.
- [10] Haugen, D. A., 1978: Effects of sampling rates and averaging periods on meteorological measurement, *4th Symp. on Meteorol. Observ. and Instrum.*, 15-18.
- [11] Roth, M., Okc, T.R. and D. G. Steyn, 1989: Velocity and temperature spectra and cospectra in an unstable suburban atmosphere, *Boundary-Layer Meteorol.*, 309-320.
- [12] Frenkiel, F. N., 1951: Frequency distribution of velocity in turbulent flow, *J. Meteorol.*, **8**, 316-320.
- [13] Sorbjan, Z., 1989: *Structure of the Atmospheric Boundary Layer*, Prentice Hall, New Jersey, 70, 134.
- [14] Panofsky, H. A. and J. A. Dutton, 1984: *Atmospheric Turbulence*, Wiley, New York, 156-173.
- [15] Kaimal, J. C., Wyngaard, J. C., Izumi, Y. and O. R. Cot, 1972: Spectral characteristics of surface layer turbulence, *Q. J. R. Meteorol. Soc.*, **98**, 563-589.
- [16] Wyngaard, J. C. and O. R. Cot, 1972: Cospectral similarity in the atmospheric surface layer, *Q. J. R. Meteorol. Soc.*, **98**, 590-603.
- [17] Hgstrm, U., 1990: Analysis of turbulence structure in the surface layer with a modified similarity formulation for near neutral conditions, *J. Atmos. Sci.*, **47**, 1949-1962.